ISSN 2347 - 3983
Volume 9. No. 7, July 2021
International Journal of Emerging Trends in Engineering Research
Available Online at http://www.warse.org/IJETER/static/pdf/file/ijeter11972021.pdf
https://doi.org/10.30534/ijeter/2021/11972021

The Diaphragm Wall Deflection Simulation Project was Tested in Ho Chi Minh City, Vietnam

Huu-Bang Tran[1], Hai-Linh Nguyen[2]
[1]Faculty of Architecture, Thu Dau Mot University, Binh Duong province, Vietnam,
bangth@tdmu.edu.vn
[2]Faculty of Architecture, Thu Dau Mot University, Binh Duong province, Vietnam,
linhnh@tdmu.edu.vn

ABSTRACT
Checking and calculating the stability of retaining walls and deep excavation are required in the design and construction of subterranean structures, particularly the DW500 reinforced concrete Wall-Plate. This is one of the most significant approaches to preventing landslides and settlement for buildings in the immediate vicinity. In fact, calculating and forecasting the DW500 retainer wall's stability and determining the influent area can provide a variety of options for reducing reinforced frame parts (retaining wall and shoring). This technology is now being explored and used for the most realistic structures in Vietnam, particularly in Ho Chi Minh City. This article uses the finite element technique (FEM – Plaxis 2D-2019) to calculate the lateral displacements, shoring, and outer foundation for the DW500 retaining wall.

Key words: Plaxis 2D, Diaphragm Wall-Plate DW500, displacement, and impact surrounding deep excavation.

1. INTRODUCTION

Raft foundations – piles are the type of foundation that combines the load carrying capacity of the rafters and pile groups [1], [2], [3], [8]. Some cases of applying pile raft foundation for high-rise buildings in the world [Table 1].

Table 1: Compile a list of projects throughout the world that use pile foundations.

Projects	Height (m), Floor	Transmission (%)		Settlement S_{max} (mm)
		Piles	Rafts	
Messeturn, Frankfurt	257m (843ft), 63th	57	42	144
Westend 1, Frankfurt	208m (682ft), 53th	49	51	120
Skyper, Frankfurt	154m (505ft), 38th	63	27	55
QV1, Perth, West Australia	163m (535ft), 40th	70	30	40
Petronas, Kuala Lampur	452m (1483ft), 88th	85	15	40

Barrette pile diaphragm walls are erected deep into the earth under the foundation to minimize soil retention and are exposed to horizontal soil movement in high-rise buildings with basements piled raft foundation and basement floor, and diaphragm wall connected with rafters and basement floor to form a system of "Pile Raft Foundation - Diaphragm Wall" (PRF-DW) [Figure 1]. Pressure during the construction of deep excavation pits and system construction of piled raft foundation and basement floor, and diaphragm wall connected with rafters and basement floor to form a system of "Pile raft foundation - Diaphragm wall".

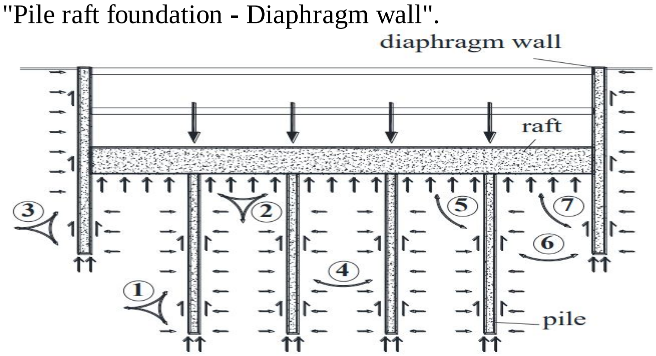

Noted: 1-Interactived pile and soil; 2- Interactived paft and soil; 3- Interactived DW and soil; 4-Interactived pile and pile; 5-Interactived paft and pile; 6-Interactived DW and pile; 7- Interactived DW and paft.

Figure 1: Interactived behavior of the nail system

Only the potential of load-carrying capacity of the rafters and piles was considered in the current research, without addressing the vertical load-carrying ability of the diaphragm wall, in the "Pile raft foundation - diaphragm wall" system, as well as the interaction impact of the diaphragm wall and the pile group in the common working model [4], [5], [6].

During the design and construction of high-rise constructions with inter-floor basements in a smart manner. The diaphragm wall of the deep excavation's horizontal displacement must be monitored. The major causes of landslides are an excavated pit diaphragm wall and adjacent structure settling, which can result in subsidence and collapse of nearby structures. The importance of neighbourhood work in accordance with building stages cannot be overstated.

In the design of deep excavations, a variety of approaches for studying diaphragm wall transverse displacement and settlement of nearby structures are employed, including analytical methods, beam methods on elastic foundations, and finite element methods (FEM). The procedure is more difficult in specific, but it produces less volatile and reliable analytical findings. (Chang Yu Ou, 2006) [7].

Other studies have found that the backdrop model employed has a significant impact on the findings of the stability and horizontal displacement analysis of the excavation pit diaphragm (Vo Phan and Ngo Duc Trung, 2015) [9]. Furthermore, the background models' input parameters have a major impact on the outcomes.

The purpose of this paper is to investigate the horizontal displacement of the basement diaphragm wall and the settlement of the road foundation in Ho Chi Minh City's District 1. Plaxis 2019 - by technique (FEM). The analysis findings provide an acceptable soil model and ground parameters to serve as a foundation for comparison with real DW500 earth retaining wall displacement monitoring, resulting in a reasonable soil model and ground parameters to serve as a basis for design work following stages.

2. PRIMARY CONTENT

2.1 Subjects for research

Work on the SJC office building was mimicked in the research. The present state of the works is as follows: The left hand side is People's Committee of District 1 (5 floors + 2 basements); on the Right there is Villa 26 Phung Khac Khoan (4 floors + 2 basements); the front is Sidewalk of Phung Khac Khoan Street and finally inside Existing SJC office (5 floors + 1 basement) [Figure 2 and Figure 3].

Figure 2. Site of the project

Figure 3. A perspective sketch of the project

2.2 Data to be entered

Earth retaining wall DW500 geological structure and parameters Table 2 and Table 3 [10][11].

Table 2: This is the first material in a Plaxis 2D model.

Material model Hardening Soft Soil					
Parameter		Layer of leveling	Letarit Sand layer	Clay and Sand layer	Clay layer
h	(m)	1	7	30	20
γ_{unsat}	(kN/m^3)	18	20.1	20.7	21.2
γ_{sat}	(kN/m^3)	18.5	20.3	21	21.2
k	(m/day)	2	0.00864	1	0.00864
E_{50}^{ref}	(kN/m^2)	8000	14000	16000	31500
E_{eod}^{ref}	(kN/m^2)	8000	14000	16000	31500
E_{ur}^{ref}	(kN/m^2)	24000	42000	48000	94500
c´	(kN/m^2)	5	15.3	5.5	40
φ´	(^{0})	20	15.72	23.7	17.2
ψ	(^{0})	0	0	0	0
ν	-	0.2	0.2	0.2	0.2
k_0	-	0.66	0.73	0.60	0.70
N_{spt}	-	0	7	16	37

Table 3: Input parameters for the DW500, Shoring and Kingpost in a Plaxis 2D model.

Parameter	Name	Value	Unit
Type of behaviour	*Material type*	*Elastic*	-
Normal stiffness	*EA*	13500000	(kN/m)
Flexural rigidity	*EI*	281250	(kNm^2/m)
Equivalent thickness	*d*	0.5	m
Poisson's ratio	*v*	0.2	-
Axial stiffnes-Shoring H400x400x13x21	*EA*	4.10^6	kN
Axial stiffnes-Kingpost H350x350x12x19	*EA*	3.10^6	kN
Spacing-Shoring	L_s	7.0	m

2.3 Techniques of construction calculation

Simulate the stages of deep excavation construction, as well as the excavation sequence based on recognized building procedures [Figure 4].

Step 1: Build a DW500 diaphragm wall using bored piles and a Kingpost.
Step 2: Start digging for the first time (Cote basement floor 1)
Step 3: Set up a shoring system for class 1 vehicles (H400).
Step 4: Return to the dirt and dig it a second time (Cote basement floor 2).
Step 5: Install layer 2 of the shoring system (2H400).
Step 6: For the third time, dig the dirt (Cote the bottom of the raft foundation).
Step 7: Basement floor 2 – concrete raft foundation
Step 8: Remove Layer 2 of the Shoring.
Step 9: Layout of the concrete basement level 1.
Step 10: Remove the first layer of shoring.

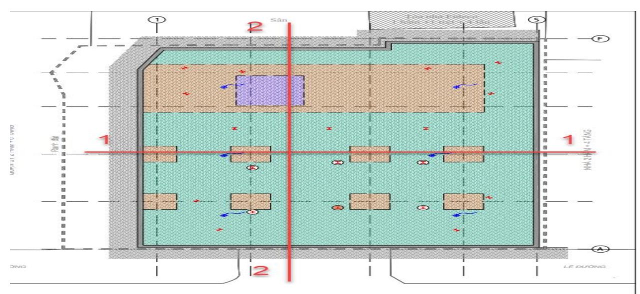

Figure 4. Sections of a Computational Model

2.3.1 Section 1 - 1 Calculation Results: The excavation depth is 9m - 9.6m and 10.9m, calculated from the bottom of tunnel B2 to the bottom of the raft foundation. The simulated load is the construction load next to it [Figure 5].

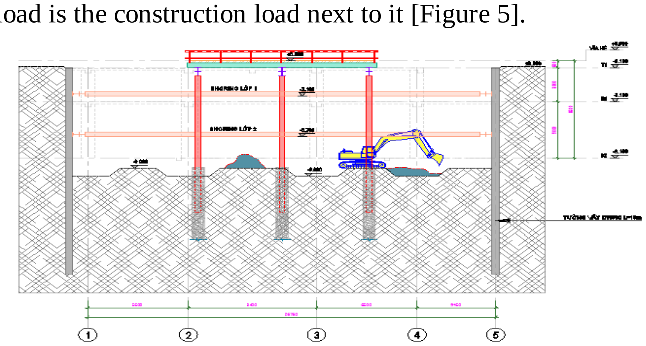

Figure 5. Section 1 – 1 Typical details

* The sequence in which the earthwork construction phases are calculated:

- Phase 1: Status of the Project;
- Phase 2: Consolidation of a building's current load;
- Phase 3: DW500 construction;
- Phase 4: For the first time, dig (basement 1);
- Phase 5: SF1.

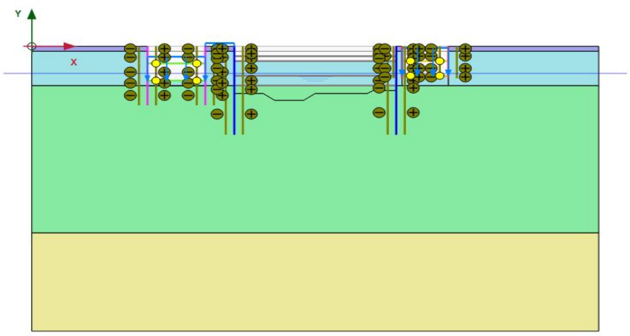

Figure 6. Simulation of a computation for digging a hole

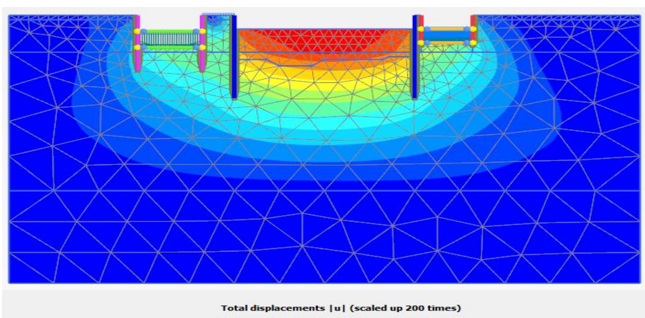

Figure 7. Displacement total

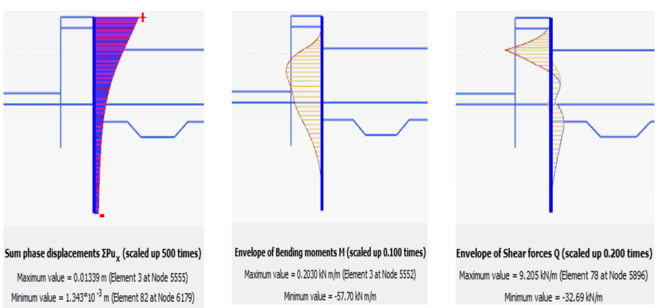

$U_x = 1.5$ *(cm)* $M_{max} = 58$ *(kNm/m)* $Q_{max} = 33$ *(kN/m)*

Figure 8. DW500 **(**People's Committee of District 1)

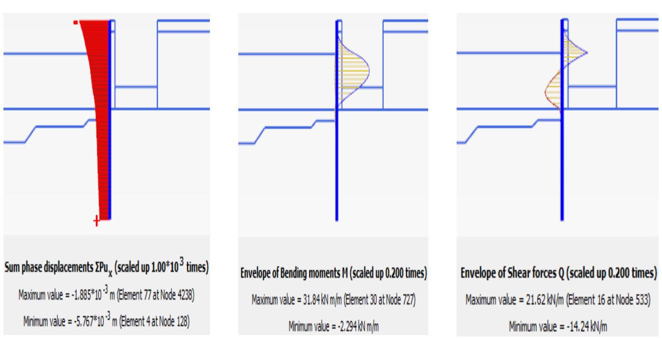

$U_x = 1$ *(cm)* $M_{max} = 32$ *(kNm/m)* $Q_{max} = 22$ *(kN/m)*

Figure 9. DW500 **(**Villa 26 Phung Khac Khoan)

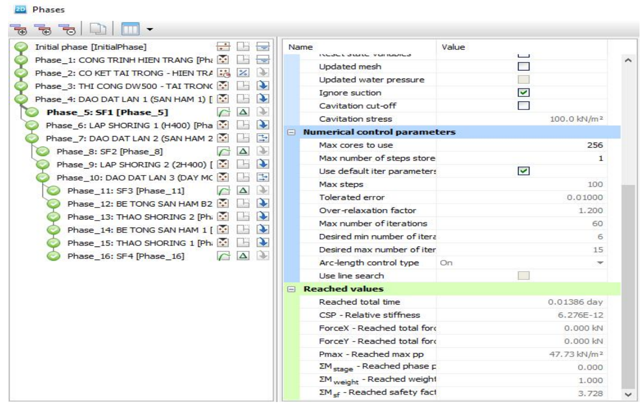

Figure 10. Reached safety fact *Msf = 3.728*

- Phase 6: Layer 1 of Mounting Shoring (H400);
- Phase 7: Digging for the second time (Teil floor 2);
- Phase 8: SF2.

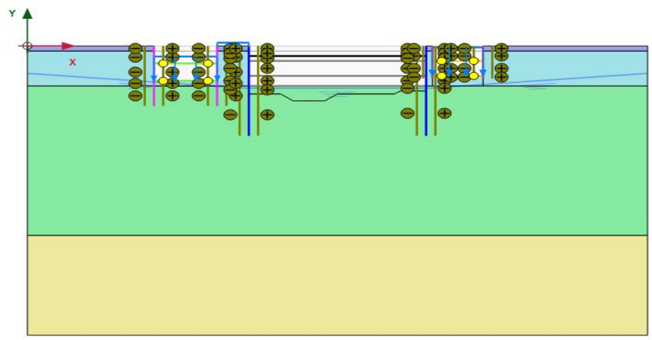

Figure 11. Simulation of a computation for digging a hole

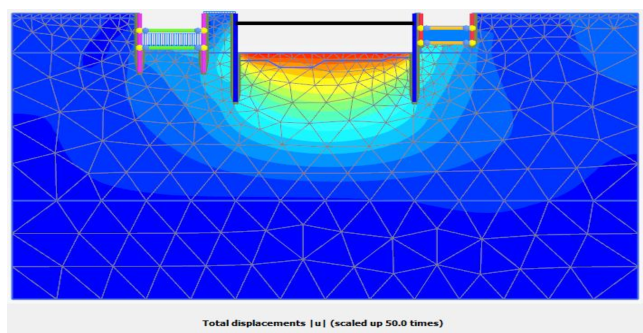

Figure 12. Displacement total

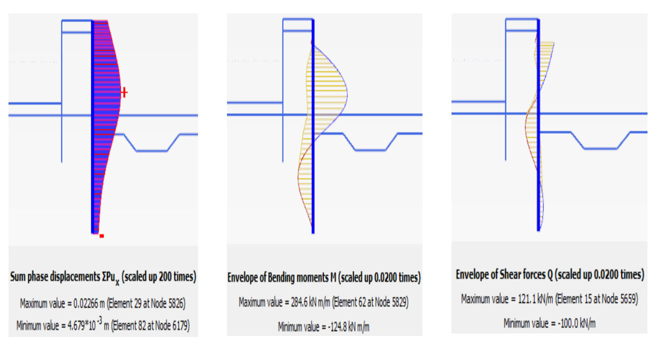

$U_x = 2.3$ *(cm)* $M_{max} = 285$ *(kNm/m)* $Q_{max} = 121$ *(kN/m)*

Figure 13. DW500 **(**People's Committee of District 1)

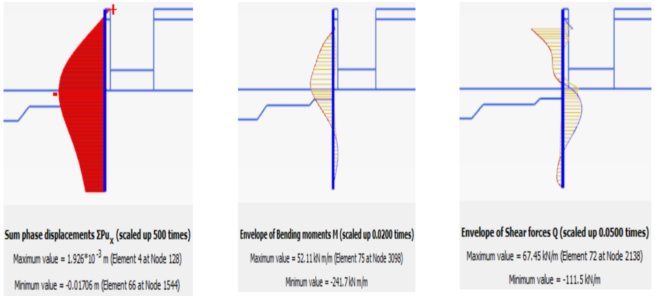

U_x = 1.7 (cm) *M_{max} = 242 (kNm/m)* *Q_{max} = 111.5 (kN/m)*

Figure 14. DW500 **(**Villa 26 Phung Khac Khoan)

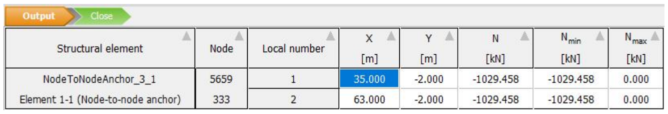

Structural element	Node	Local number	X [m]	Y [m]	N [kN]	N_{min} [kN]	N_{max} [kN]
NodeToNodeAnchor_3_1	5659	1	35.000	-2.000	-1029.458	-1029.458	0.000
Element 1-1 (Node-to-node anchor)	333	2	63.000	-2.000	-1029.458	-1029.458	0.000

Figure 15. Shoring strut system response class 1 result

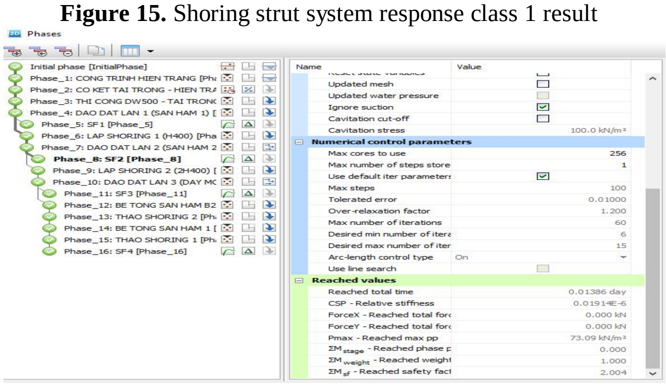

Figure 16. Reached safety fact *Msf = 2.004*

- Phase 9: Layer 2 of Mounting Shoring (2H400);
- Phase 10: Digging No. 3 (bottom of raft foundation);
- Phase 11: SF3.
- Phase 12: Filling the basement floor with concrete;
- Phase 13: Remove the second layer of shoring (2H400).
- Phase 14: Basement floor 1 is made of concrete;
- Phase 15: Remove the first layer of shoring (H400);
- Phase 16: SF4.

*** Remarks:** Internal force and the maximum value of DW500 displacement are added together.

People's Committee of District 1	U_x	3.4 (cm)
	M_{max}	334 (kNm/m)
	Q_{max}	184 (kN/m)
Villa 26 Phung Khac Khoan	U_x	2.3 (cm)
	M_{max}	257 (kNm/m)
	Q_{max}	181 (kN/m)
1st grade shoring struts	$L_{Spacing}$ = 7 m	1118 (kN)
2nd grade shoring struts	$L_{Spacing}$ = 7 m	1930 (kN)

2.3.2 Section 2 - 2 Calculation Results:

Section 2 - 2: The section estimated from the bottom of the basement floor B2 to the bottom of the raft foundation, with excavation depths of 9 - 9.6 m and 10.9 m. Construction live loads and nearby construction loads are examples of simulated loads. The author would like to summarize the findings.

*** Remarks:** Internal force and the maximum value of DW500 displacement are added together.

Existing SJC office	U_x	4 (cm)
	M_{max}	399 (kNm/m)
	Q_{max}	218 (kN/m)
Sidewalk of Phung Khac Khoan Street	U_x	4.1 (cm)
	M_{max}	420 (kNm/m)
	Q_{max}	226 (kN/m)
1st grade shoring struts	$L_{Spacing}$ = 7 m	1870 (kN)
2nd grade shoring struts	$L_{Spacing}$ = 7 m	2267 (kN)

2.4 Graoundwater flow

2.4.1 Section 1 - 1 Calculation Results

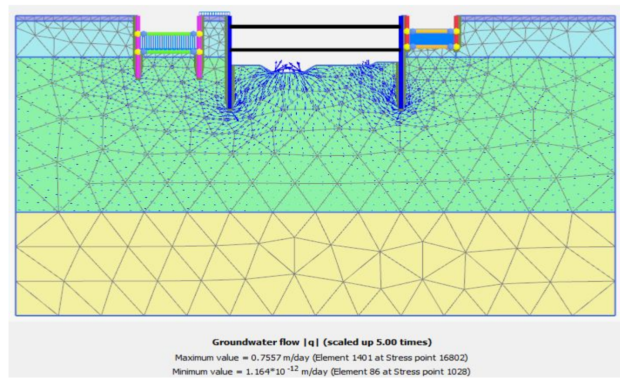

Figure 17. The seepage stress during the excavation stage to the raft foundation's bottom

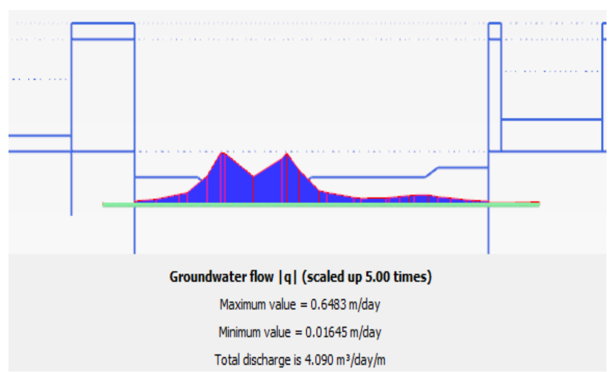

Figure 18. The result of water flowing through the excavation pit's bottom.

2.4.2 Section 2 - 2 Calculation Results

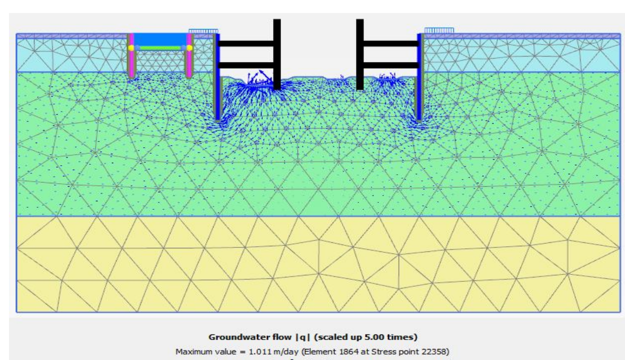

Figure 19. The seepage stress during the excavation stage to the raft foundation's bottom

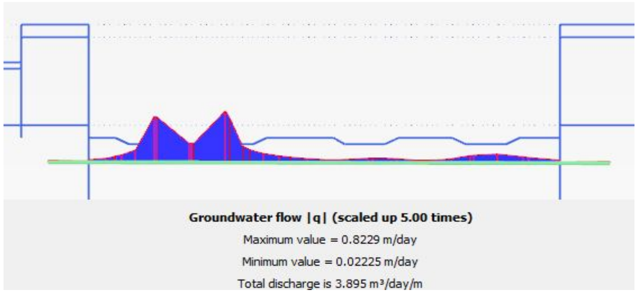

Figure 20. The result of water flowing through the excavation pit's bottom.

*** Remarks:**

- Total discharge is Q = 4.1 (m^3/day/m).
- The total amount of water that seeps into the structure Q_{sum} = 4.1*(36+28) = 262.4 (m^3/day/m).
- The number of wells is estimated to be four, with an effective radius of around 15 meters and a capacity of 5-7 horsepower. As a result, 1 pump has the following daily pumping capacity: Q_a = 262.4 / 4 = 67 (m^3/day).

2.5 Examine the impact of the excavation pit

2.5.1 Influence Sphere

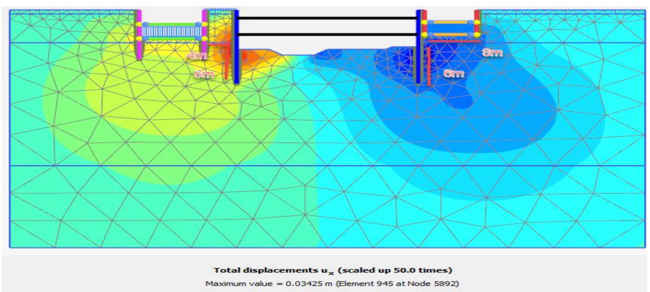

Figure 21. Section 1 - 1 of the Influence Sphere

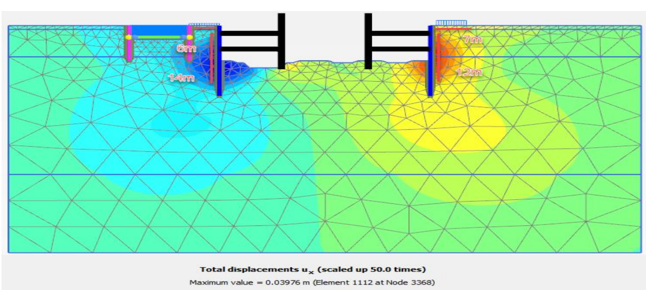

Figure 22. Section 2 - 2 of the Influence Sphere

2.5.2 The following is the foundation for assessing the outcomes of the calculations

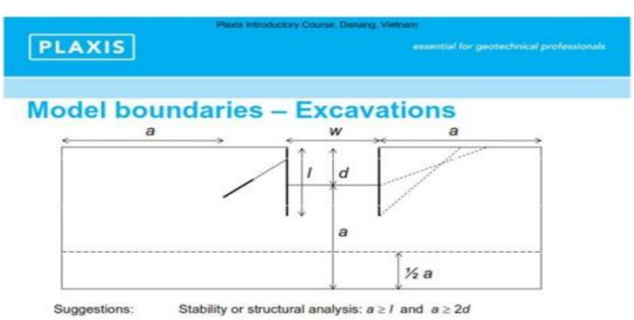

Figure 23. Plaxis 2D Introductory Course

*** Remarks:**

- The greatest extent of effect from the position of the excavation border to neighboring structures and existing infrastructure is 8m, based on the displacement of the surrounding earth during the excavation.
- The deep excavation problem's impact margin is generally more than or equal to 2 times the excavation depth, or greater than or equal to 1 time the excavation's diaphragm wall length. This indicates that the greatest effect range is R = 2 x H = 2 x 9 = 18m or R = 1 x L = 1 x 18 = 18m from the border of the excavation to the surrounding ground.

3. CONCLUSIONS

- The bearing capacity is ensured by the DW500 diaphragm wall system, anti-Shoring system, and side beams.
- The diaphragm wall People's Committee of District 1 expects DW500 as the maximum horizontal displacement: 3.4 (cm).
- Villa 26 Phung Khac Khoan is diaphragm wall anticipates a maximum horizontal displacement of DW500: 2.3 (cm).
- The maximum horizontal displacement estimated for the current SJC office DW500 diaphragm wall: 4.0 (cm).
- The diaphragm wall DW500 on Phung Khac Khoan Street's Sidewalk is projected to shift the greatest horizontally: 4.1 (cm).
- The number of wells is estimated to be four, with an effective radius of around 15 meters and a capacity of 5-7 horsepower. As a result, 1 pump has the following daily pumping capacity: Q_a = 262.4 / 4 = 67 (m^3/day).
- The impact margin in basement construction earthworks is restricted to 18 meters.
- Proposed diaphragm wall displacement limit for DW500: $U_{xmax} = H_{digging}/150$ = 9/150 = 6 (cm).
- The horizontal displacement of the DW500 diaphragm wall system must be monitored during the excavation operation. Simultaneously, frequent monitoring of subsidence and tilting of surrounding works is carried out.
- If a deviation from the warning level is very significant, the appropriate parties must be alerted so that prompt action may be taken.
- The following are some recommended preventative measures: (Stop excavation activity if backfilling is required; Increase the stability of the strut system throughout the excavation process; Maintain command of the situation. To go on to the following phases, you'll need to design and calculate the safety reinforcement. The shoring strut system must be built completely according to the plans).

REFERENCES

1. Randolph, M.F. **Design methods for pile groups and piled rafts.** *In: Proc. 13th international conference on soil mechanics and foundation engineering*, Vol. 5, pp. 61–82, New Delhi, India. 1994.
2. P. Clancy and M.F. Randolph. **Simple design tools for piled raft foundations**. *Géotechnique*, Vol. 46 Issue 2, pp. 313-328, June 1996.

3. Poulos H.G. **Piled raft foundations: design and applications.** *Géotechnique*, Vol. 51, Issue 2, pp. 95-113, March 2001.
4. Katzenbach, R., et al. **High-Rise Buildings In Germany. Soil-Structure Interaction of Deep Foundation.** *In: Proc. 5th. Int. Conf. on Case Histories in Geotechnical Engineering*, New York, NY, Apri 2004, pp.13-17.
5. Sales MM, Small JC, Poulos HG and Harry G. Poulos. **Compensated piled rafts in Clayey soils: Behaviour, measurements, and predictions.** *Can Geotech. J*. Vol. 47, 2010, pp. 327-345.
6. Kumar A., Choudhury D. and Katzenbach R.,: **Effect of Earthquake on Combined Pile-Raft Foundation**. *International Journal of Geomechanics* ASCE, ISSN 1532-3641; 2016. pp. 1-16.
7. Chang-Yu Ou. (2006), **Deep Excavation - Theory and Practice, Taylor & Francis Group**, *London, UK*.
8. Nguyen Nhut Nhat, Le Ba Vinh and To Le Huong. **Analysis of interaction effects of the diaphragm wall and the pile group in Piled raft foundations - Diaphragm wall,** *Viet Nam Geotechnical Journal*. Vol 4, 2020, pp.51-60.
9. Ngo Duc Trung (2015) **To stabilize a deep excavation, a displacement study of a retaining wall was performed**. *(Viet Nam National University Ho Chi Minh City).*
10. Plaxis 2D V8.5 (2019). *Tutorial Manual*.
11. Van-Vinh Nguyen, Thi-Kieu Pham and Huu-Bang Tran. **Evaluation of Response Modification Factor of Multiple Story Steel Buildings**. *International Journal of Emerging Trends in Engineering Research.* ISSN 2347-3983, Vol. 8. No. 4, April 2020, pp. 1342-1348.